coatings

Article

Effects of Strontium-Hydroxyapatite Mediated Active Compounds from *Hippocampus Kuda* Bleeler (HKB) on Osteogenesis

Chengyong Li [1,2,*] , Qiong Yuan [3] , Lei He [1] , Zhong-Ji Qian [1,2] , Chunxia Zhou [2,3,*] and Pengzhi Hong [2,3,*]

[1] School of Chemistry and Environment, Guangdong Ocean University, Zhanjiang 524088, China; airyhelei@163.com (L.H.); zjqian78@163.com (Z.-J.Q.)
[2] Shenzhen Institute of Guangdong Ocean University, Shenzhen 518108, China
[3] College of Food Science and Technology, Guangdong Ocean University, Zhanjiang 524088, China; yuanqiong0415@163.com
[*] Correspondence: cyli_ocean@163.com (C.L.); chunxia.zhou@163.com (C.Z.); hongpengzhi@126.com (P.H.); Tel.: +86-759-238-3636 (C.L.)

check for updates

Abstract: Porous hydroxyapatite as a drug carrier is very popular and has many clinical applications. However, traditional hydroxyapatite materials have limited osteogenic capacity. Therefore, the development of a new hydroxyapatite drug delivery system is essential for bone tissue engineering. In this study, the metal element Sr was used to replace Ca, and the SrHA microspheres were successfully prepared by hydrothermal reaction. Scanning electron microscopy (SEM), X-ray diffraction (XRD), and X-ray photoelectron spectroscopy (XPS) were used to characterize SrHA (strontium-doped hydroxyapatite) microspheres obtained from hydrothermal reaction conditions. In addition, the drug utility was enhanced by loading the marine active compound 1-(5-bromo-2-hydroxy-4-methoxyphenyl)-ethanone (HKB). Furthermore, after co-culture with preosteoblasts, experiments indicated that HKB/SrHA composite microspheres had a more significant effect on the proliferation and differentiation of cells compared to pure SrHA. These HKB/SrHA composite microspheres may be applied to the drug delivery system of bone tissue repair.

Keywords: hydroxyapatite; strontium; *hippocampus kuda* bleeler; MC3T3-E1

1. Introduction

In recent years, osteoporosis, bone defects, and osteomyelitis have become one of the chronic diseases that plague the health of middle-aged and elderly people in various countries. Research on such diseases has always been a hot spot for scholars. The balance between bone formation of osteoblasts in tissues and bone resorption of osteoclasts is a key factor affecting bone strength and integrity [1,2]. Due to some external factors such as age, heredity, and lifestyle, the balance between bone resorption and formation is disrupted, resulting in osteoporosis due to the loss of bone mass. Currently, basic supplements such as calcium [3], vitamin D [4,5] and related derivatives, bone loss inhibitors and bone formation promoters play an important role in the treatment of osteoporosis [6]. Osteon loss inhibitors such as estrogen can reduce the production of osteoclasts [7], and bisphosphonates inhibit osteoclast activity [8], thereby inhibiting bone resorption and preventing bone loss. Previous studies have shown that Chinese herbal extracts of epimedium can effectively promote the proliferation and differentiation of osteoblasts, accelerate cell maturation, promote cell mineralization, accelerate bone formation, and prevent osteoporosis [9]. Polygonatum polysaccharide can promote osteogenic differentiation of mouse bone marrow mesenchymal stem cells through the

Wnt/β-catenin signaling pathway [10]. The marine-derived mother-of-peaside glycosaminoglycan also significantly promoted differentiation and mineralization of Sprague Dawley (SD) neonatal rat calvarial osteoblasts but did not promote cell proliferation [11]. However, there are certain limitations in the treatment of pharmaceutical preparations or active preparations, such as that the effect is not obvious, or the side effects are large.

As the main inorganic component in teeth and bones, hydroxyapatite has superior biocompatibility and biological activity [12]. Hydroxyapatite is widely used as one of biocoatings. Coating nano-hydroxyapatite on the surface of titanium promotes angiogenesis and inhibits inflammatory responses [13]. Carbon fiber, polycaprolactone (PCL) surface coating hydroxyapatite provides a suitable 3D environment for the adhesion, proliferation, and differentiation of osteoblasts and significantly improves the performance of scaffold materials [14,15]. Moreover, hydroxyapatite has many applications in drug delivery systems due to its structural characteristics. For example, local delivery of alendronate and growth factor BMP-2 was achieved by custom hydroxyapatite microspheres [16]. Hydroxyapatite–magnetite–multi-walled carbon nanotube (MWCNT) nanocomposites have been used in drug delivery systems for their excellent biocompatibility [17]. In order to prevent the occurrence of mplant-associated infection, gentamicin was loaded with the mesoporous hydroxyapatite microspheres to the implant site for sustained release [18]. Biomimetic hydroxyapatite–drug nanocrystals can be directly used as a potential bone substitute with antitumor drug delivery properties [19]. These targeted drug delivery systems are highly demanding on hydroxyapatite itself. From the nature of the material, it is important to select the optimal hydroxyapatite synthesis conditions. There are several other methods cited to improve the biological activity of hydroxyapatite, such as the loading of biologically active molecules, doping active trace elements, etc. The Zn–HA composite structure not only maintains an excellent biocompatibility of hydroxyapatite but also has a superior antibacterial effect and can be applied to oral orthopedics [20]. Mg–HA is used as filler for femoral defects. In vitro experiments have shown that its composite structure has superior bone conductivity and resorption than commercial stoichiometric HA granulate [21]. Recently, the newly developed drug for the treatment of osteoporosis, strontium (Sr) ranelate, was shown to have a dual role in stimulating osteoblast differentiation and inhibiting osteoclast activity and bone resorption, which can reduce the incidence of fractures in patients with osteoporosis [22]. In addition, studies have shown that the amelioration of hydroxyapatite osteogenesis can be achieved by substituting Sr for Ca [23,24]. Therefore, we prepared SrHA microspheres (strontium-doped hydroxyapatite) as the substrate material for the following experiments.

Hippocampus kuda Bleeler is a highly valuable Chinese herbal medicine with high medicinal, nourishing, and ornamental value. Its main chemical components include amino acids, active peptides, steroids, fatty acids, and various trace elements, with a wide range of pharmacological effects and exact clinical efficacy [25,26]. The main pharmacological effects of active compounds isolated from the hippocampus are anti-inflammatory, anti-oxidation, and antitumor. Currently, there are few reports on bone tissue repair [27].

Herein, we successfully developed SrHA microspheres and loaded with active compound 1-(5-bromo-2-hydroxy-methoxyphenyl)-ethanone (HKB) derived from Hippocampus. After that, we studied the effects of different groups of samples on preosteoblasts in in vivo experiments. And indicated that an HKB/SrHA composite microsphere could significantly promote the proliferation and differentiation of MC3T3-E1 cells. Thus, it provided a promising therapeutic strategy against osteoporosis in future clinical applications.

2. Materials and Methods

2.1. Extraction of 1-(5-Bromo-2-hydroxy-4-methoxyphenyl) Ethanone (HKB)

The active compound HKB was obtained from previous research by our group. The lyophilized hippocampal powder was crudely extracted with MeOH and partitioned with n-hexane/EtOAc/

MeOH in sequence, then purified using silica gel column. The structural identification of HKB was obtained though electron ionization mass spectrometry (EIMS) spectra (Agilent7890A/5975C, USA).

2.2. Synthesis and Characterization of Strontium-Doped Hydroxyapatite Microspheres

A total of 0.2221 g of $Sr(NO_3)_2$ and 8.0174 g of $Ca(NO_3)_2$ were thoroughly dissolved in 70 mL of deionized water, and then 2.7732 g of $NH_4H_2PO_4$ was added and stirred well. A total of 6.3062 g of urea was dissolved in the above solution, and the pH was adjusted to 2.41–2.45 with 0.1 mol/L HNO_3 solution. The resulting solution was then transferred to a 20 mL autoclave and heated at 120 °C for 72 h and naturally cooled to room temperature. After the hydrothermal reaction, the resulting suspension was washed three times with absolute ethanol and distilled water. SrHA porous microspheres were obtained and dried at 50 °C for 24 h and then stored in 70% ethanol for use. Since the prepared SrHA sample is almost insoluble, the phase, crystallinity, and elemental combination of the SrHA microspheres was analyzed by X-ray diffractometry (Rigaku MiniFlex 600, Tokyo, Japan) and X-ray photoelectron spectroscopy (Thermo Scientific K-Alpha$^+$, USA), and the microstructure was observed by scanning electron microscopy (Hitachi S-4800, Tokyo, Japan).

2.3. Preparation of HKB/SrHA Composite Microspheres

The prepared SrHA was dried at 60 °C. A total of 10 mmol/L of hippocampus extract HKB was dropwise to the surface of 0.01 g of SrHA and air-dried at room temperature. After HKB was completely attached to the SrHA microspheres, the amount of HKB loaded was measured by a depletion method. Since the optimal concentration of HKB was 20 μmol/L and SrHA was 60 μmol/L in co-culture experiments with MC3T3-E1 cells (Figure 3a,b), the amount of SrHA and loading compound HKB are in accordance with the above concentration ratio when prepared HKB/SrHA composite.

2.4. Culture of MC3T3-E1

The pre-osteoblast MC3T3-E1 was inoculated into a culture flask at a density of 2×10^4 per mL and cultured in minimum essential medium (MEM) with 10% fetal bovine serum and 1% double antibody (penicillin-streptomycin), then placed in a 37 °C, 5% CO_2 cell culture incubator.

2.5. Cell Attachment Experiment (Fluorescence Staining)

Pre-osteoblasts grown to logarithmic growth phase were seeded in 24-well plates (HKB, SrHA, HKB/SrHA) that had been added and placed in cell culture incubator after 6 h. The original medium was aspirated and washed repeatedly for three times with PBS to remove unattached cells, and the concentration of 4% paraformaldehyde fixative was fixed at room temperature for 10 min. The paraformaldehyde solution was removed and washed twice with PBS, then stained with fluorescent dye 4′, 6-Diamidino-2-Phenylindole (DAPI) (100 ng/mL) for 3 min in the dark, washed 3 times with PBS, and placed under a fluorescent inverted microscope to observe the pre-osteoblasts.

2.6. Examination of Cell Proliferation (MTT Method)

The pre-osteoblasts grown in the logarithmic growth phase were inoculated into a 24-well plate, and after 1 day of culture, the complete medium (without serum) was replaced, and the samples (HKB, SrHA, HKB/SrHA) were added, and the culture was continued for 1 day or 3 days. The supernatant was discarded, 200 μL of 3-(4,5-dimethyl-2-thiazolyl)-2,5-diphenyl-2-*H*-tetrazolium bromide (MTT) solution was added to each well, and the culture was stopped after further incubation at 37 °C for 4 h, and the culture solution in the well was aspirated. A total of 200 μL of dimethyl sulfoxide (DMSO) was added to each well and shaken at a low speed for 10 min on a shaker to dissolve the formed formazan crystals. The optical density (OD) value was read at 490 nm in an enzyme-linked immunosorbent assay.

2.7. Determination of Alkaline Phosphatase (ALP)

The pre-osteoblasts that grew vigorously in the logarithmic growth phase were selected and inoculated into a 24-well plate. After 1 day of culture, the new medium was replaced to contain 1 mol/L β-glycerophosphate, 10 mmol/L dexamethasone, 50 mg/mL ascorbic acid, 10% fetal bovine serum, 1% double antibody. At the same time, samples (HKB, SrHA, HKB/SrHA) were added to induce differentiation for 3 days and 7 days. The culture solution was discarded and gently washed repeatedly with PBS buffer for 2 to 3 times to eliminate the influence of serum components on the measurement results. Then, 0.1% TritonX-100 cell lysate was added dropwise to freeze-thaw the cells. After 40 min in an ice bath, p-nitrophenyl phosphate solution (p-NPP) was added to the lysate, and the temperature was 37 °C. After 1 h of incubation, the OD value was read at a wavelength of 405 nm by an enzyme-linked immunosorbent assay.

2.8. Statistics

All data were evaluated for significance by t-tests with *p*-values of 0.05 and expressed as mean ± SEM (standard error of the mean).

3. Results

3.1. Characterization of Strontium-Doped Hydroxyapatite Microspheres

Figure 1 shows the SEM and XRD diffraction patterns of SrHA obtained after 72 h reaction at 120 °C. The hydrothermally produced SrHA is a microsphere structure formed by a plurality of short rods. The diameter of the microspheres is approximately 11 μm (Figure 1a). Figure 1b,c shows the XRD patterns of the synthesized sample SrHA microspheres and pure HA microspheres. According to the standard diffraction spectrum JCPDS (09-0432) HA diffraction pattern, the diffraction peak positions are basically the same, and the peak at 31.8° and 33° is the strongest characteristic peak of hydroxyapatite. Figure 1c clearly confirms that the corresponding peaks of the synthetic SrHA microspheres significantly shift to a lower degree when compared to the pure HA. This indicates an increase in the lattice constant, which may be due to the replacement of the Ca ions by a bigger atomic diameter of Sr. Quantitative X-ray photoelectron spectroscopy (XPS) analysis was performed on the SrHA. Typical survey and high-resolution spectra are presented in Figure 1c–f. The survey spectrum of the SrHA also contains the Sr3d peak in addition to the Ca2p, P2p peaks, confirming the presence of the strontium.
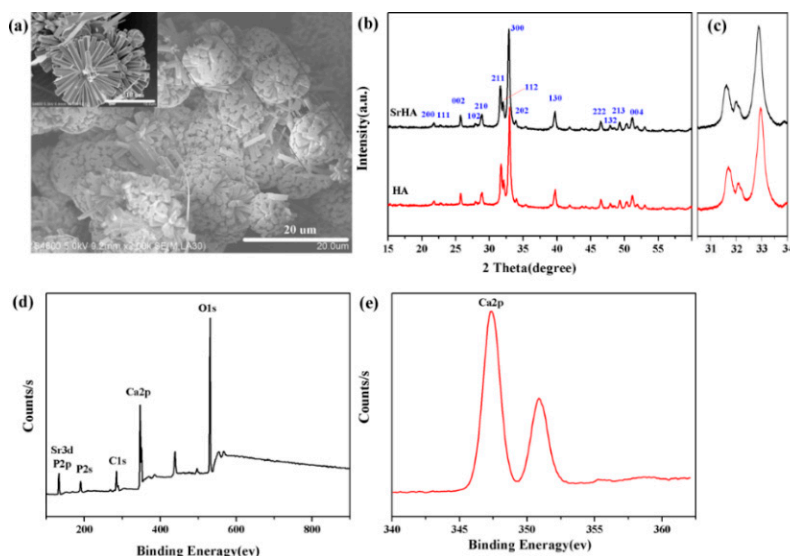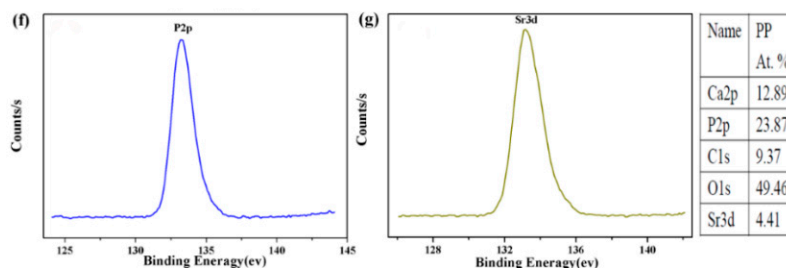

Figure 1. *Cont.*

Figure 1. (**a**) SEM and (**b**,**c**) XRD pattern of SrHA sample and the control HA sample. (**d**) X-ray photoelectron spectroscopy (XPS) survey scan and high-resolution XPS spectra of the (**e**) Ca2p peak, (**f**) P2p peak, and (**g**) Sr3d peak peaks of the SrHA.

Figure 2 shows the FTIR spectra of HKB, SrHA, and HKB/SrHA, respectively. Peaks at 565 cm^{-1}, 605 cm^{-1}, and 1040 cm^{-1} are characteristic peaks of $P0_4^{3-}$. At 1455 cm^{-1} and 1414 cm^{-1}, the peak of CO_3^{2-} splits, showing two absorption peaks, which are different from the single peak in carbonate. This is an important sign of CO_3^{2-} entry into the apatite structure. The 1600 cm^{-1}, 1580 cm^{-1}, 1450 cm^{-1}, and 1500 cm^{-1} peaks were attributed to the ring breathing vibration of the benzene, which was consistent with the EIMS spectra results. By comparing the infrared spectra of HKB/SrHA and pure SrHA, it was confirmed that the compound HKB was successfully loaded into SrHA.
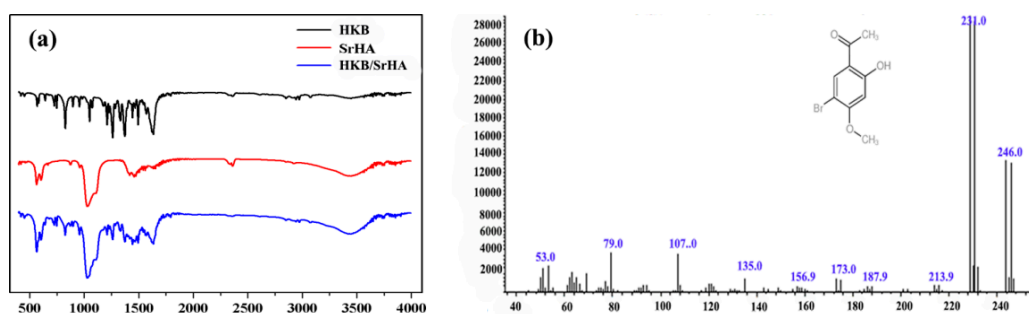
Figure 2. (**a**) FTIR spectra of 1-(5-bromo-2-hydroxy-4-methoxyphenyl)-ethanone (HKB), SrHA and HKB/ SrHA; (**b**) EIMS spectra data for HKB.

*3.2. Screening of Optimal Concentrations of HKB and SrHA Co-Cultured with MC3T3-E1 Cells*

The cellular activity MC3T3-E1 cultured with compound HKB and SrHA microspheres was determined by MTT assay. MTT is reduced to colorimetric formazan crystals by mitochondrial energy metabolism of amber dehydrogenase in living cells, and its OD value can directly reflect the number of viable cells. According to Figure 3a, HKB has the highest activity at a concentration of 20 μmol/L. Figure 3b shows that when the concentration of hydroxyapatite is 60 μmol/L, it has a significant effect on the proliferation of pre-osteoblasts.
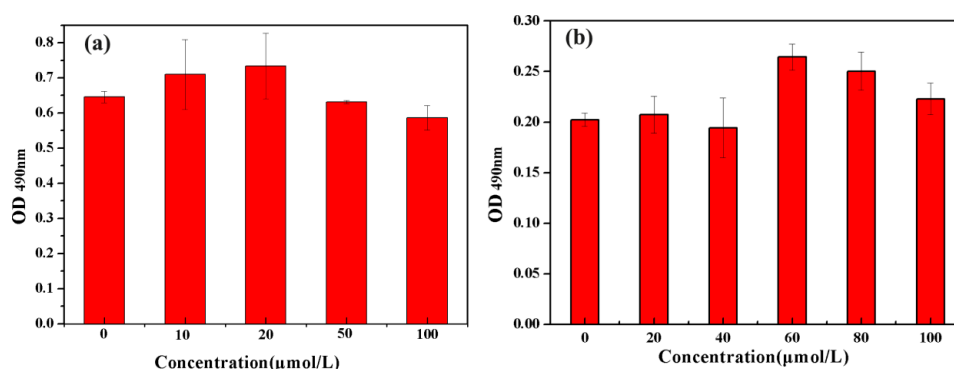
Figure 3. Cellular activity of MC3T3-E1 cultured with different concentrations of (**a**) HKB and (**b**) SrHA.

### 3.3. Evaluation of Adhesion Ability of Pre-Osteoblasts under Different Conditions

The fluorescence staining of cells is shown in Figure 4. MC3T3-E1 cells were stained by DAPI fluorescent dye, which reflects the early attachment of cells. DAPI fluorescent dye can strongly bind to DNA through cell membrane for staining of living cells. Figure 4a–d shows the difference in the number of cells attached to each of the samples (Control, HKB, SrHA, HKB/SrHA). These images suggest that the HKB/SrHA group has a higher viable cell density than the other groups (Figure 4e). The pure SrHA group was significantly higher than the control group, indicating that SrHA has good osteoblast induction ability. SrHA as a coating material can increase the surface roughness of the substrate, which has a great effect on the early viscosity of osteoblasts. In addition, the large specific surface area of SrHA microspheres laid the foundation for its good drug-loading capacity. Compared to the pure SrHA group, HKB has a pronounced cell adhesion promoting ability. It is further explained that HKB derived from the hippocampus has superior biocompatibility. This may be related to the phenolic hydroxyl groups of the chemical structure of HKB [28,29].
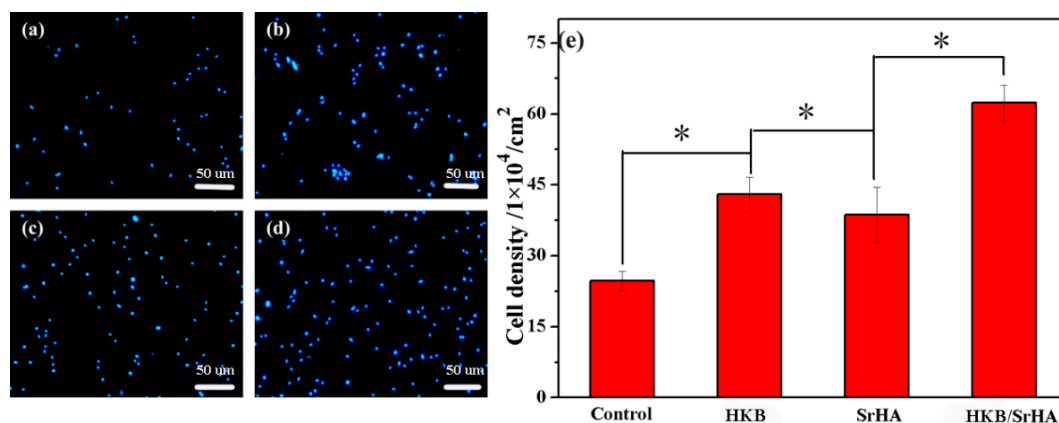
Figure 4. Fluorescence staining of preosteoblasts attachment observations: (**a**) Control, (**b**) HKB, (**c**) SrHA, (**d**) HKB/SrHA, (**e**) cell density of adhering cells cultured with different samples. * $p < 0.05$.

3.4. Effect of HKB/SrHA on Proliferation

After studying the effects of each group of samples on the early adhesion of MC3T3-E1, the cell proliferation value was obtained with MTT assay after cultured 1 day and 3 days. There was no significant difference between the HKB and SrHA group at day 1. However, after 3 days of inoculation, it was found that each group of samples had significant cell proliferation, and the HKB/SrHA group had better cell growth (Figure 5).
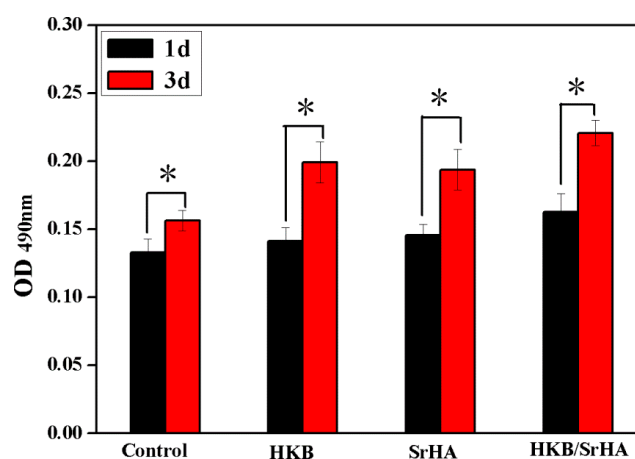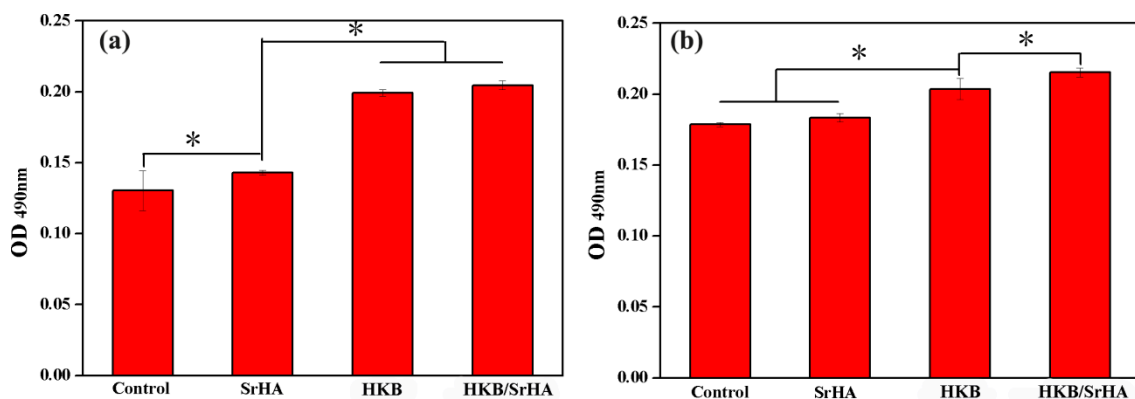

Figure 5. Proliferation of MC3T3-EI cultured in each group for 1 and 3 days. * $p < 0.05$.

3.5. Effect of HKB/SrHA on ALP Activity

Differentiation on the various samples was characterized using ALP as an early phase marker. In view of the synergistic effect of SrHA and HKB, which has effective biological activity in osteogenic differentiation of MC3T3-E1, we believe that these HKB/SrHA microspheres can be applied for an effective osteoinductive platform, by triggering the generation of ALP and a mineralized matrix. Thence, to further assess osteoblast differentiation on HKB/SrHA microspheres, alkaline phosphatase activity was also investigated. Figure 6 shows ALP activity of MC3T3-E1, which was cultured in normal medium as a control group, seeded to different samples (Control, SrHA, HKB, HKB/SrHA) at 3 and 7 days. The test results showed that osteoblasts could successfully differentiate and synthesize alkaline phosphatase in different sample groups. Compared to that of the pure SrHA and pure HKB group, a significant improvement in peak ALP activity was observed owing to the addition of HKB into SrHA (Figure 6a). Concomitantly, as a graph showing the longer ALP activity of osteoblasts (Figure 6b), it was clearly demonstrated that the ALP activity of the HKB/SrHA group was significantly higher after 7 days culture.

Figure 6. Proliferation of MC3T3-E1 cultured in each group for 3 and 7 days. (**a**) 3 days; (**b**) 7 days; * $p < 0.05$.

4. Conclusions

In the present work, the active compound HKB derived from the hippocampus was loaded into SrHA to prepare HKB/SrHA microspheres with higher biological activity, which was not previously reported. The SrHA were characterized using XRD, SEM, and XPS. It was further proved through in vitro experiments that HKB/SrHA composite microspheres have the obvious ability of osteoblast proliferation and differentiation because of the synergistic effect of SrHA and HKB. Therefore, HKB/SrHA composite microspheres could be applied to the drug delivery system of bone tissue repair.

References

1.　　Kim, H.J.; Minashima, T.; Mccarthy, E.F.; Winkles, J.A.; Kirsch, T. Progressive ankylosis protein (ANK) in osteoblasts and osteoclasts controls bone formation and bone remodeling. *J. Bone Miner. Res.* **2010**, *25*, 1771–1783. [CrossRef] [PubMed]

2.　Zhai, Y.; Li, Y.; Wang, Y.; Cui, J.; Feng, K.; Kong, X.; Chen, L. Psoralidin, a prenylated coumestan, as a novel anti-osteoporosis candidate to enhance bone formation of osteoblasts and decrease bone resorption of osteoclasts. *Eur. J. Pharmacol.* **2017**, *801*, 62–71. [CrossRef] [PubMed]

3.　Pro-Risquez, A.; Harris, S.S.; Song, L.; Rudicel, S.; Barnewolt, B.; Dawson-Hughes, B. Calcium supplement and osteoporosis medication use in women and men with recent fractures. *Osteoporos. Int.* **2004**, *15*, 689–694. [CrossRef] [PubMed]

4.　Tian, Y.; Li, W.; Hai, G.; Zhang, Y. Effect of calcium supplement on superoxide dismutase and malonaldehyde of disuse osteoporosis in young rats. *J. Hyg. Res.* **2003**, *32*, 49–50.

5.　Sanfelix-Genovés, J.; Gil-Guillén, V.F.; Orozco-Beltran, D.; Giner-Ruiz, V.; Pertusa-Martínez, S.; Reig-Moya, B.; Carratalá, C. Determinant Factors of Osteoporosis Patients' Reported Therapeutic Adherence to Calcium and/or Vitamin D Supplements. *Drugs Aging* **2009**, *26*, 861–869. [CrossRef] [PubMed]

6.　Jin, G.; Aobulikasimu, A.; Piao, J.; Aibibula, Z.; Koga, D.; Sato, S.; Ochi, H.; Tsuji, K.; Nakabayashi, T.; Miyata, T. A small-moleculePAI-1 inhibitor prevents bone loss by stimulating bone formation in a murine estrogen deficiency-induced osteoporosis model. *Febs. Open Biol.* **2018**, *8*, 523–532. [CrossRef] [PubMed]

7.　García, P.V.; Robinson, L.J.; Borysenko, C.W.; Lehmann, T.; Kalla, S.E.; Blair, H.C. Negative regulation of RANKL-induced osteoclastic differentiation in RAW264.7 Cells by estrogen and phytoestrogens. *J. Biol. Chem.* **2005**, *280*, 13720–13727. [CrossRef]

8.　Carano, A.; Teitelbaum, S.L.; Konsek, J.D.; Schlesinger, P.H.; Blair, H.C. Bisphosphonates directly inhibit the bone resorption activity of isolated avian osteoclasts in vitro. *J. Clin. Investig.* **1990**, *85*, 456–461. [CrossRef]

9.　Yin, X.X.; Chen, Z.Q.; Dang, G.T.; Ma, Q.J.; Liu, Z.J. Effects of Epimedium pubescens icariine on proliferation and differentiation of human osteoblasts. *China J. Chin. Mater. Med.* **2005**, *30*, 289–291.

10.　Zong, S.; Zeng, G.; Zou, B.; Li, K.; Fang, Y.; Lu, L.; Xiao, D.; Zhang, Z. Effects of Polygonatum sibiricum polysaccharide on the osteogenic differentiation of bone mesenchymal stem cells in mice. *Int. J. Clin. Exp. Pathol.* **2015**, *8*, 6169–6180.

11.　Kocabey, S.; Ceylan, H.; Tekinay, A.B.; Guler, M.O. Glycosaminoglycan mimetic peptide nanofibers promote mineralization by osteogenic cells. *Acta Biomater.* **2013**, *9*, 9075–9085. [CrossRef] [PubMed]

12.　Roy, D.M.; Linnehan, S.K. Hydroxyapatite formed from Coral Skeletal Carbonate by Hydrothermal Exchange. *Nature* **1974**, *247*, 220–222. [CrossRef] [PubMed]

13.　Bai, L.; Liu, Y.; Du, Z.; Weng, Z.; Yao, W.; Zhang, X.; Huang, X.; Yao, X.; Crawford, R.; Hang, R. Differential effect of hydroxyapatite nano-particle versus nano-rod decorated titanium micro-surface on osseointegration. *Acta Biomater.* **2018**, *76*, 344–358. [CrossRef] [PubMed]

14.　Sandeman, S.R.; Jeffery, H.; Howell, C.A.; Smith, M.; Mikhalovsky, S.V.; Lloyd, A.W. The in vitro corneal biocompatibility of hydroxyapatite coated carbon mesh. *Biomaterials* **2009**, *30*, 3143–3149. [CrossRef]

15.　Milovac, D.; Gamboa-Martínez, T.C.; Ivankovic, M.; Ferrer, G.G.; Ivankovic, H. PCL-coated hydroxyapatite scaffold derived from cuttlefish bone: In vitro cell culture studies. *Mater. Sci. Eng. C Mater. Biol. Appl.* **2014**, *42*, 264–272. [CrossRef] [PubMed]

16.　Lee, J.H.; Ko, I.H.; Jeon, S.-H.; Chae, J.-H.; Chang, J.H. Micro-structured hydroxyapatite microspheres for local delivery of alendronate and BMP-2 carriers. *Mater. Lett.* **2013**, *105*, 136–139. [CrossRef]

17.　Alessandro, P.; Daniela, I.; Silvia, P.; Monica, M.; Anna, T.; Signorino, G. Hydroxyapatite-magnetite-MWCNT nanocomposite as a biocompatible multifunctional drug delivery system for bone tissue engineering. *Nanotechnology* **2014**, *25*, 425701.

18.　Guo, Y.J.; Long, T.; Chen, W.; Ning, C.Q.; Zhu, Z.A.; Guo, Y.P. Bactericidal property and biocompatibility of gentamicin-loaded mesoporous carbonated hydroxyapatite microspheres. *Mater. Sci. Eng. C Mater. Biol. Appl.* **2013**, *33*, 3583–3591. [CrossRef]

19.　Palazzo, B.; Iafisco, M.; Laforgia, M.; Margiotta, N.; Natile, G.; Bianchi, C.L.; Walsh, D.; Mann, S.; Roveri, N. Biomimetic Hydroxyapatite–Drug Nanocrystals as Potential Bone Substitutes with Antitumor Drug Delivery Properties. *Adv. Funct. Mater.* **2010**, *17*, 2180–2188. [CrossRef]

20.　Prodan, D.; Moldovan, M.; Prejmerean, C.; Silaghi-Dumitrescu, L.; Boboia, S.; Popescu, V.; Pascalau, V.; Molea, A.; Diana, L.; Perhaiâ£A, I. Synthesis and Characterization of an Experimental Zn-Hydroxyapatite Powders with Application in Dentistry. *Key Eng. Mater.* **2013**, *587*, 43–51. [CrossRef]

21.　Landi, E.; Logroscino, G.; Proietti, L.; Tampieri, A.; Sandri, M.; Sprio, S. Biomimetic Mg-substituted hydroxyapatite: From synthesis to in vivo behaviour. *J. Mater. Sci. Mater. Med.* **2008**, *19*, 239–247. [CrossRef]

22. Atkins, G.; Welldon, K.P.; Findlay, D. Strontium ranelate treatment of human primary osteoblasts promotes an osteocyte-like phenotype while eliciting an osteoprotegerin response. *Osteoporos. Int.* **2009**, *20*, 653–664. [CrossRef]

23. Zhang, C.; Cheng, Z.; Yang, P.; Xu, Z.; Peng, C.; Li, G.; Lin, J. Architectures of strontium hydroxyapatite microspheres: Solvothermal synthesis and luminescence properties. *Langmuir* **2009**, *25*, 13591–13598. [CrossRef]

24. Lin, K.; Liu, P.; Wei, L.; Zou, Z.; Zhang, W.; Qian, Y.; Shen, Y.; Chang, J. Strontium substituted hydroxyapatite porous microspheres: Surfactant-free hydrothermal synthesis, enhanced biological response and sustained drug release. *Chem. Eng. J.* **2013**, *222*, 49–59. [CrossRef]

25. Sanaye, S.V.; Pise, N.M.; Pawar, A.P.; Parab, P.P.; Sreepada, R.A.; Pawar, H.B.; Revankar, A.D. Evaluation of antioxidant activities in captive-bred cultured yellow seahorse, Hippocampus kuda (Bleeker, 1852). *Aquaculture* **2014**, *434*, 100–107. [CrossRef]

26. Sun, D.; Wu, S.; Jing, C.; Zhang, N.; Liang, D.; Xu, A. Identification, synthesis and characterization of a novel antimicrobial peptide HKPLP derived from Hippocampus kuda Bleeker. *J. Antibiot.* **2012**, *65*, 117–121. [CrossRef]

27. Kang, N.; Kim, S.Y.; Rho, S.; Ko, J.Y.; Jeon, Y.J. Anti-fatigue activity of a mixture of seahorse (Hippocampus abdominalis) hydrolysate and red ginseng. *Fish. Aquat. Sci.* **2017**, *20*, 3–10. [CrossRef]

28. Nordberg, A.; Antoni, P.; Montañez, M.I.; Hult, A.; Von, H.H.; Malkoch, M. Highly adhesive phenolic compounds as interfacial primers for bone fracture fixations. *ACS Appl. Mater. Interfaces* **2010**, *2*, 654–657. [CrossRef]

29. Manna, C.; Della, R.F.; Cucciolla, V.; Borriello, A.; D'Angelo, S.; Galletti, P.; Zappia, V. Biological effects of hydroxytyrosol, a polyphenol from olive oil endowed with antioxidant activity. *Adv. Exp. Med. Biol.* **1999**, *472*, 115–130.